A topologically complex cytoplasm enables inflation-based escape from a gravity trap

Adam G. Larson [1], Rahul Chajwa [1], Hongquan Li [1] Manu Prakash* [1]
[1] *Department of Bioengineering, Stanford University, Stanford CA 94305 USA and*
* *To whom correspondence should be addressed: manup@stanford.edu*
(Dated: August 18, 2022)

Abstract

Living cells evolve under specific ecological conditions. The mass of our planet setting a constant gravitational pull and its daily rotation on its axis setting a circadian rhythm are two examples of universal ecological parameters that shape the physiology of every living creature on earth. In the ocean, gravity plays a critical role in shaping the life history of phytoplankton with vast diversity of size and cell geometries all depending on light to survive while gravity is pulling them down. In order to survive, these organisms must evolve means to navigate a vertically stratified ocean. Here we present how cellular topology can enable sinking, rising, and levitation dynamics of seemingly non-motile cells in the open ocean. By studying the bio-luminescent dinoflagellate *Pyrocystis noctiluca*, we discover how rapid inflation dynamics regulates cell size and buoyancy in coordination to its cell cycle. Live-cell light-sheet imaging reveals a (n-genus) toroidal cytoplasm that enables this rapid inflation of overall cell volume over 5 fold in 15 minutes without dilution of cytoplasmic contents. Here we present combined field and lab measurements with system modeling to build a general framework for how non-motile plankton can escape the gravitational sedimentation trap, and how precise control of cell size becomes essential to survival. Our work on cellular levitation emphasizes the critical role of studying cell and evolutionary biology in its planetary context.

Introduction

Plankton, *the wanderers*, get their namesake from a reliance on the movement of waters they inhabit to sustain themselves. Although ocean currents partly dictate plankton distribution; organisms evolved for billions of years in the ocean to navigate a vertically stratified ecosystem, from large colonies [52] to single cells [2, 10]. Life in the ocean encounters two boundary conditions, that of the sunlit ocean surface and that of the darkness at the ocean floor[6, 23, 43]. Between the two limits; gradients of temperature[29, 36], pressure[51, 59], salinity, nutrients, and elemental composition[17]act as fundamental drivers for biochemical adaptation in these planktonic cells.

For photosynthetic organisms the dilemma of vertical positioning in the ocean stems from a need to maintain some proximity to sunlight (euphotic zone) while also gaining access to nutrients that might only be accessible in deeper waters [67, 68]. Since the eukaryotic cytoplasm is usually 5 to 10% heavier than seawater, this induces a constant risk of sinking below the euphotic zone and losing the ability to photosynthesize [13]. Indeed much of the larger phytoplankton collected below 150 meters are found without visible chloroplasts [25]. However, in the oligotrophic (low nutrient) waters that constitute over 50% of the total ocean, nutrients such as nitrogen are only slowly supplied to the well-mixed surface layer [3, 21]. Despite this, organisms comprising over 40% of total oceanic production thrive in these waters [3, 24]. These plankton evolved to sense the physical and chemical stratification and navigate up and down between the surface and these nutrient enriched deeper waters. Terrestrial cells, including our own, still harbor salts in composition and concentrations similar to seawater [9]. Maintaining and managing this composition has remained one of the most energetically costly investments cells achieve [55].

Above a length scale given by comparing sedimentation velocity and energy scale of velocity fluctuations in the ocean, metabolic and reproductive processes must factor in the density of biochemical products and their influence on sedimentation. We term the fundamental limit of sinking below the habitable zone for a given phytoplankton via sedimentation as a "gravitational trap". A cell must maintain station, at least temporarily, at depths that are sunlit while somehow fulfilling a demand for nutrients that are often limited close to the surface. To resolve this paradox, if a cell chooses to undergo vertical long-distance migration, it compensates for passive sinking by actively rising for progeny to not be generationally increasing depth and sedimenting to the ocean floor.

To highlight this paradox further, consider a spherical cell of radius r and cytoplasmic fluid of density ρ_c suspended in ambient seawater with density ρ_{sw} and dynamic viscosity μ. In a regime where viscous forces dominate over inertial forces for a suspended cell, sedimentation dynamics is governed by the Stokes Equation [61] giving rise to a simple relationship between cell size, cell density, and sedimentation velocity

$$\mathbf{u_z} = \frac{2r^2\mathbf{g}(\rho_c - \rho_{sw})}{9\mu}, \tag{1}$$

where the gravity direction $\mathbf{g}$ is aligned with the - z-axis and homogeneity and isotropy are assumed in the horizontal $x - y$ plane. This simple relationship provides a link between cellular physiology(cell size r, cell density ρ_c), ecology (defined by the density of seawater as a function of depth $\rho_{sw}(z)$) and cell behavior

(either positive or negative sedimentation velocity).

As effective cell density (ρ_c) is often 5-10% higher than that of ρ_{sw}, this implies the cell must actively regulate effective cell density to execute upward motion at some point within its life cycle[4, 13, 27] or else sink to the bottom of a water column. Beyond upwelling dynamics that depend on external conditions, in principle, a cell could internally change both r and ρ_c as a function of cell cycle; thus regulating cellular position in the water column as a function of where a cell is in its life cycle. Cell growth will generate organic mass and build energy reserves. Furthermore, the cell will interact with the ambient seawater for nutrient exchange and osmoregulation. Although these parameters can change throughout the life of a single cell, a closed life-cycle also implies the recursive occurrence of specific cell size (radius) and cell composition/density at a particular time point during the cycle. The above closed constraints provide tight bounds on where a passively sinking/rising cell can be found during a certain cell stage. In this simple example, sedimentation provides a framework linking internal (behavioral) and external (environmental) parameters governing how a cell can optimize ecophysiological conditions throughout its life cycle.

The incredible diversity in planktonic form display numerous solutions to a drifting life under a constant gravitational pull[45, 60]. Although swimming based ciliary motility is common amongst plankton, many single-celled phytoplankton move across vast length scales in the ocean without a typical motile organelle such as flagella or cilia. Among these include diatoms such as *Coscinodiscus bouvet*, *Rhizosolenia castracanei*, and *Ethmodiscus rex*, as well as the dinoflagellates *Pyrocystis noctiluca*, *P. lunella* and *P. fusiformis*. These cells regularly navigate 10 to 100's of meters across the vertical dimension of the ocean[25, 32, 44, 66]. How do these single cells lacking any obvious propulsion organelles migrate lengths hundreds of thousands times their size while maintaining cellular physiology?

One common strategy is believed to utilize peculiarly large vacuoles with chemical ballast to help achieve lift [32]. Many studies have postulated possible cellular mechanisms behind this activity [5, 32, 54, 64]. For *Pyrocystis noctiluca* specifically, the cell is hypothesized to alter its buoyant mass through the regulation of the composition and concentration of molecules within its bladder. Its abnormally low pH of 3.5 is also implicated through sequestration of ammonium salts which carry a large specific volume , a strategy also employed by a large family of teuthoid squid [16, 18]. However, replication challenges this buoyancy strategy by re-appropriating many of the proposed mechanisms while disrupting cytoskeletal networks, nuclear architecture, and transcriptional programs. Unlike some differentiated cells, single-celled organisms have no choice but to undergo this dramatic rearrangement to reproduce. For plankton, whose size and shape are intimately tied to controlling position in the water column, this can become an existential challenge. How single cells integrate these changes physiologically remains unknown.

Here we explore how cellular architecture and geometry of *Pyrocystis noctiluca* enable long-distance migration of this non-motile single cell. To approach this question we tracked actively migrating *Pyrocystis noctiluca* cells in the field using a vertical tracking microscope to concurrently measure cell morphology while generating a macro-scale vertical migration trajectory. This confirmed the ability of these large 500µm cells to move upward at speeds of over a meter per hour while maintaining the ability to reach depths of more than 100 meters in the open ocean. These multi-scale microscopy measurements also revealed dramatic shape and size changes in the cell body of migrating *Pyrocystis noctiluca* cells that appeared to correlate with vertical trajectories. Using stable lab cultures we imaged an entire life-cycle of these single cells in lab conditions (constant temperature, 12 hour light cycle) which revealed a remarkably rapid (15min) and large (3-6 fold) scale "inflation" event that serves to quickly decrease a cell's sinking rate. With live-cell light-sheet imaging, we uncover a unique cellular topology (n-genus torus) that enables this single cell to dilate and expand rapidly to increase its overall cell volume without diluting its cytoplasmic contents. Finally, by integrating field and lab measurements with mathematical modeling, we present a holistic model to suggest how this extraordinary feat helps these sinking organisms evade a gravitational trap, providing a critical limit on maximum cell density in a vertically stratified ocean.

Results

Cell migration in the open ocean

To capture single-cell motility behavior of the dinoflagellate *Pyrocystis noctiluca* vertically migrating in the ocean we collected cells 100km off the Hawaiian Island archipelago and recorded trajectories in a custom built scale-free vertical tracking microscope [35] on board the research vessel *Kilo Moana* during the Hawaiian Ocean Time-series cruise *HOT317*(Fig. 1A). The cells were captured at known depth using CTD (Conductivity, Temperature, and Depth) triggered rosette bottles and quickly transferred to the annular stage. To quantify motility vectors and velocities of Pyrocystis we used this seawater-filled wheel as a stage, where upward or downward movements of the object are compensated by stage rotation in the opposite direction using a closed-loop tracking system. This constitutes a "hydrodynamic treadmill" for microscale objects(Fig. 1B) [35]. A 'virtual-depth' for the object can be assigned from net angular displacement and radial position while sub-cellular morphology is recorded using microscope optics.

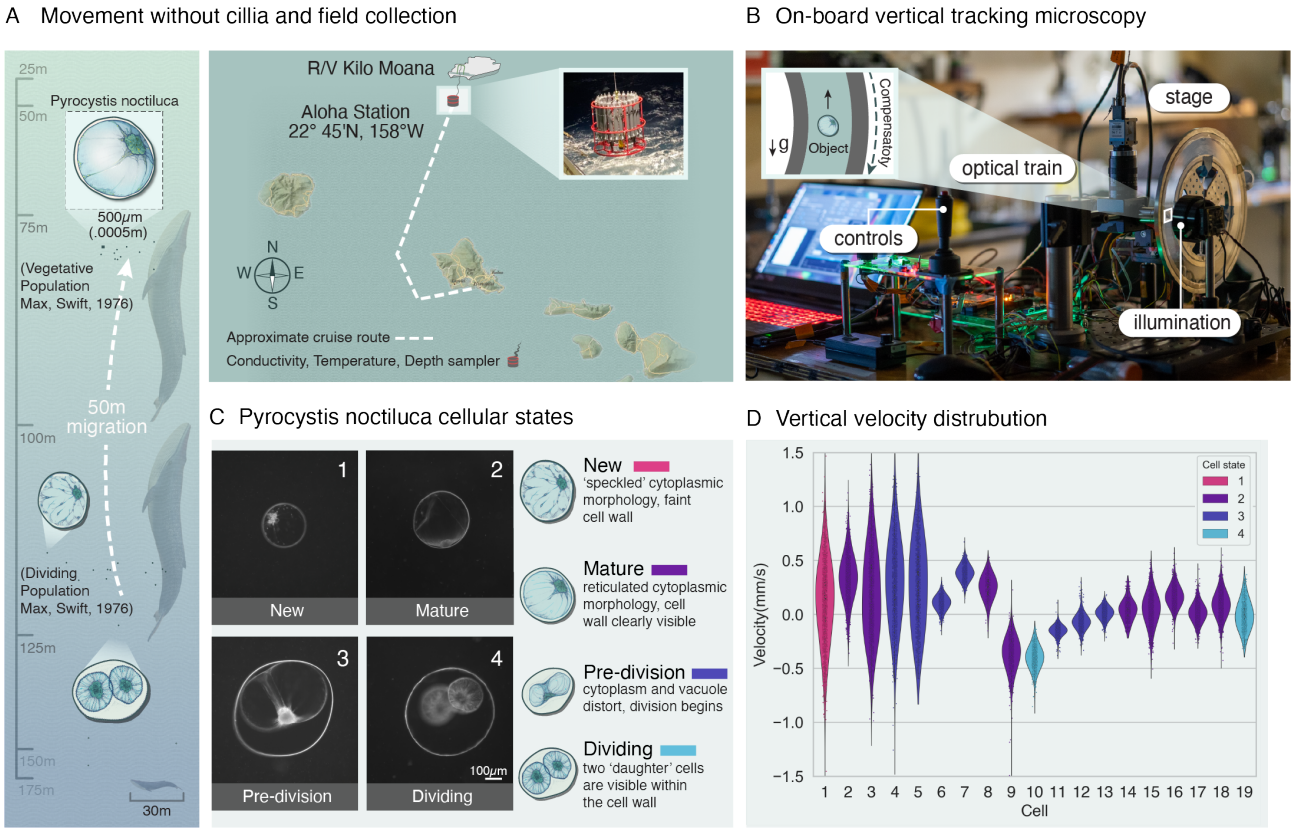

FIG. 1. **Field velocity measurements of a vertically migrating cell**.Pyrocystis noctiluca was collected during the Hawaii Ocean Timeseries (HOT317) cruise, encountered in deep waters, enabling us to make the first sedimentation velocity (behavioral) tracks of cells captured and imaged under field conditions. A)Pyrocystis noctiluca undergoes a vertical migration of over 50m within the lower euphotic zone with dividing cell populations found 25-55m below mature cells. Whale bar refers to average length of a Blue Whale(Balaenoptera musculus). Cells were collected 100km off the Hawaiian Archipelago on board the RV Kilo Moana using either a CTD rosette or net. B)Cells were immediately sorted then loaded into the tracking microscope on board the vessel, using the seawater filled wheel as a stage. C) Pyrocystis cells can be binned according to cell state, from (1)newly formed cells,(2) mature cells, (3)cells beginning to undergo mitosis, and (4) cells with two daughter cells present.D)60 second vignettes from individual cell tracks in the 'gravity machine' display both positive and negative buoyancy as reflected in relative sedimentation velocities. Most of the observed mature Pyrocystis cells display positive buoyancy and move upward in the water column. Pyrocystis cells undergoing division, with two daughter cells present(4), were observed to move downward in the water column.

We recovered several Pyrocystis cells from a CTD pull at a depth of 75 meters, confirming earlier reports of its residency at the lower euphotic zone [64]. However, foul conditions precluded reproducible long term access from the CTD. We later relied on organisms from plankton tows performed at a depth of 25-35 meters. Unlike diatoms, radiozoa, and other observed cells, many mature (vegetative) *Pyrocystis noctiluca* cells were observed to rise(Movie S1). Confirming earlier reports, dividing cells instead displayed negative buoyancy(sinking), while mature cells displayed negative, neutral(nearly suspended), to positive buoyancy(rising) [64](Fig. 1C,D, Movie S1). Positively buoyant cells moved upward at rates nearing 0.4mm/s. This corresponds to a vertical displacement of 10's of meters per day. A puzzle therefore arises: without up-welling flows, how do cells that presumably lack a self-propulsion mechanism control long-distance vertical migrations?

Since the vertical tracking microscope provides both sedimentation velocity and cellular state via tracking microscopy, we looked for a correlation between the two. Indeed, we find that cell-state (new, mature, pre-division, or dividing) correlates with sedimentation (upward or downward) behavior, as reported previously[63, 64](Fig. 1C,D). To understand this cell migration behavior in its environmental context we need to map cell state to physiological parameters. For example, cells might maintain different effective cell densities during different parts of their metabolic cycle and use that to beneficially position themselves in the vertically stratified ecosystem.

Cell inflation and density measurements

Pyrocystis noctiluca is a large spherical (slightly prolate) cell(Fig. 2C). The cell is highly pigmented and decorated with plastids that are highly mobile(Fig. S1B, C, Movie S2).

In the context of sedimentation, it is useful to consider the cell morphology in context of two separate components - cytoplasm and vacuole volume and density - where effective cell density can be written as

$$\rho_{eff} = \rho_{cy}\frac{V_{cy}}{V_c} + \rho_{vac}\frac{V_{vac}}{V_c} \tag{2}$$

where ρ_{cy}, ρ_{vac}, ρ_{eff} are cytoplasmic, vacuole and effective cell density, and V_{cy}, V_{vac}, V_c are the volume of cytoplasm, vacuole, and the cell respectively - while all of the above parameters might be a function of where a cell is in its cell cycle.

To understand how this state/morphology change would influence sedimentation behavior we imaged Pyrocystis cells throughout an entire replicative cycle. In lab-based day/night settings, we find that on average, cells divide roughly every 7 days in a temperature and light-controlled environment (Movie S3). Long-term time-lapse imaging reveals the dynamic nature and associated topology of cytoplasmic networks that appear as thin strands; transporting pigmented plastids to and from the cell periphery with each day/night transition (Movie S3). This results in a network that vastly increases surface area during sun-lit hours and decreases nuclear to periphery distance during darkness.

Surprisingly, immediately following division, daughter cells undergo a large and rapid inflation event increasing the total volume of the cell over 5 fold in 10-15 minutes(Fig. 2A, B). This observation sets up another dilemma, how can a single cell cope with a near order of magnitude volume increase in under 10 minutes? Such rapid and large scale cellular swelling can have catastrophic consequences on canonical cell physiology; diluting biochemical interactions, distorting membrane morphology, and causing global metabolic disturbances. Mitochondrial distortion, endoplasmic reticulum dilation, and aggregation of chromatin will considerably strain cell functions [40]. How do *Pyrocystis noctiluca* cells successfully incorporate this event, and what are the associated consequences to their behavior? Cellular growth is a process that is normally calibrated to general metabolic timelines allowing for protein production and accumulation of energy reserves [48]. This suggests such an anomalous inflation-driven growth process would likely have evolved to achieve some benefit within the life history of this dinoflagellate.

We first address the question of behavior change associated with rapid cell inflation. Inflation rapidly changes effective cell size denoted by cell radius r and can impact effective cellular density ρ_c, depending on the contents of newly added volume. Using lab cultures, we directly measure how cell division regulates sedimentation behavior in Pyrocystis by visualizing cell division events in the vertical tracking microscope(Fig. 2D,E). Cells with 2 daughter cells within, sediment at rates around -0.2mm/s. After the outer thecal breakdown, the two daughter cells separate and begin to inflate. Associated with this inflation is a rapid decrease in cell sedimentation velocity from 0.2mm/s to 0.1mm/s over the 10 minutes of volume increase. In the open ocean, populations of dividing Pyrocystis cells are 50 meters below the density maximum for vegetative cells, near the bottom of the euphotic zone [64]. As described in equation 1, sedimentation velocity is directly proportional to the product of a square of cell radius and effective cell density. Thus this decrease in sedimentation velocity as cell radius increases implies that the effective cellular density must decrease dramatically. A cell needing to rapidly decrease sinking velocity could thus employ such a strategy to avoid prolonged residence in low-light conditions after a free-fall during cell division where any bladder ballast is vastly reduced.

Cellular topology

Because the inflation process appears to be integrated into Pyrocystis's life cycle, we wanted to explore how cell physiology might cope with such rapid cell inflation without diluting cellular cytoplasm. Thus we visualize individual Pyrocystis cells at high temporal and spatial resolution with a light-sheet microscope. We used quantitative fluorescent microscopy to extract spatial characteristics and architecture of this cell. Volumetric microscopy clearly shows the majority of the cell actually consists of a large central vacuole taking up over 80% of the total internal volume. Surrounding the vacuole, and transecting through it, is a reticulated network containing cytoplasmic fluid which connects the nucleus with the periphery. We hypothesized that this cellular architecture and topology plays a critical role in a cell surviving a fast ballooning event. Next, we imaged the cells under a transmission electron microscope where this network is revealed to be a membrane-bound filamentous network containing not only pigmented chloroplasts, but a highly jammed mixture of various organelles(Fig. 3C,G, S3). Because these fibers are filled with plastids, we know that this cytoplasmic network should be highly autofluorescent. This was further confirmed by wide-field fluorescence images using red and far-red excitation(Fig. S1D, E, F). Quantitative light-sheet micrographs of a mature cell reveal this fluorescence marking the pigmented cytoplasm to make up less than 5% of a calculated total cell volume(Fig. 3B, S3A). In a pre-division daughter cell, this cytoplasm makes up significantly more cell volume(Fig. 3B, S3A). As we image live cells undergoing the inflation process we observe the total cell volume increase several-fold, however the quantification of cytoplasmic signal reveals only a modest increase during the process(Fig. 3B, S3A, Movie S6).

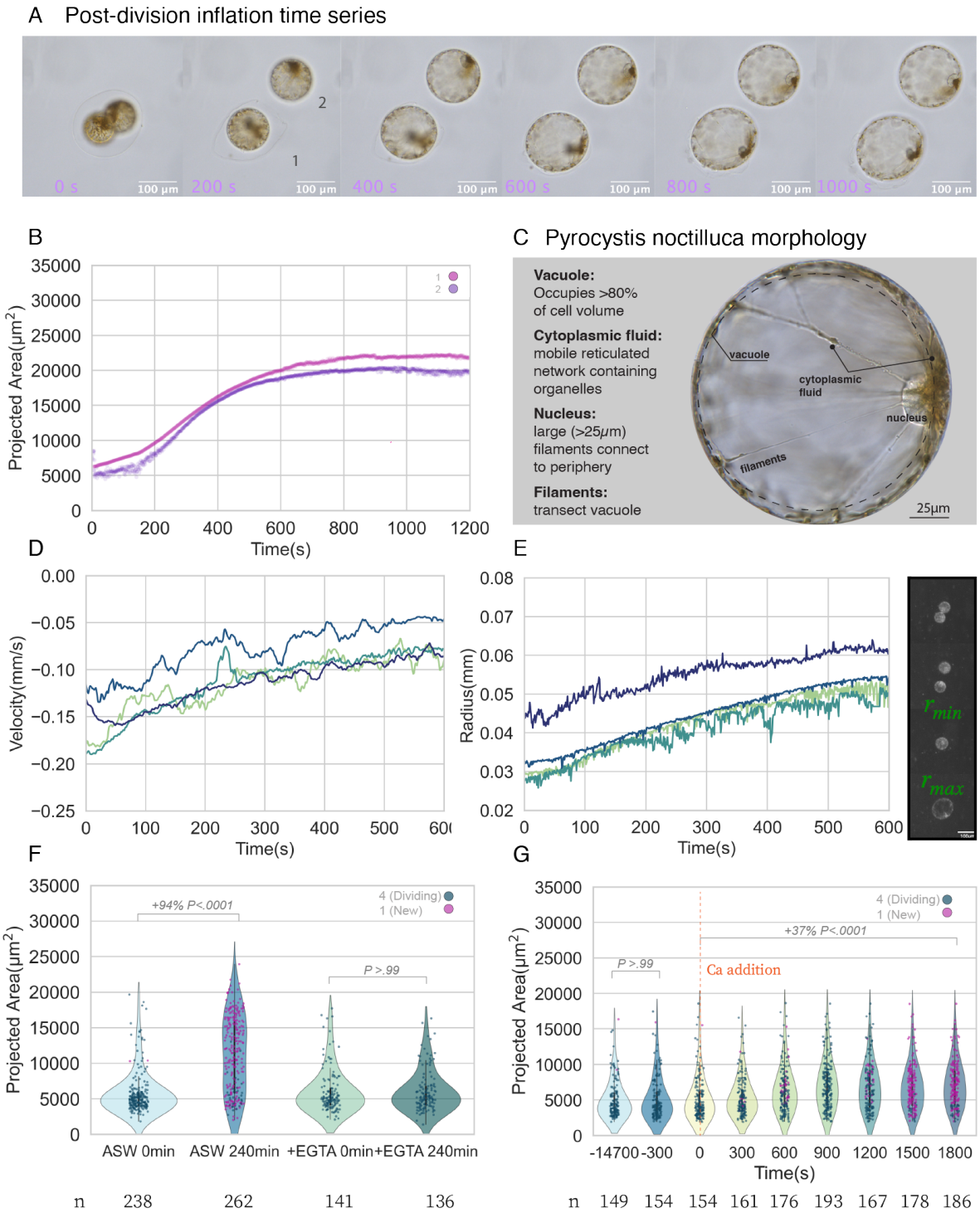

FIG. 2. **Triggered cellular inflation as a means of motility**.A,B)Post-division, daughter cells undergo an expansion event increasing their area over 2.5 fold in 15 minutes. C)Anatomy of Pyrocystis noctiluca. This rather large cell (500μm in the wild, 200 μm in culture) contains a large vacuole surrounded by an outer cell wall. Membrane threads contain motile cytoplasmic material distributed throughout the cell and transecting through it. D,E)Vertical tracks from individual division events in the gravity machine show a concomitant decrease in sedimentation velocity as the cell radius increases. F) Counts of dividing cells in the 4 hours post-daylight transition reveal the inflation event to be inhibited by addition of the calcium chelator EGTA. G)Calcium starved cells are still viable, as cells grown in artificial seawater without calcium undergo expansion on addition of 2mM calcium to the media.

The above imaging modalities reveal a novel architecture for this cell. The cell's cytoplasm, containing its metabolic machinery, exists as a reticulated n-torus manifold that is topologically entangled with the vacuole via membrane tunnels that traverse the vacuole volume several times. This unique cellular architecture presents novel constraints on the cell. Firstly, this topologically complex cytoplasmic network resolves the paradox of dilution due to inflation, since as the cell expands, the reticulated network stretches allowing the vacuole to expand with no net gain of cytoplasmic volume. Since the total mass of the cytoplasm remains conserved during inflation, the cytoplasmic contents do not undergo dilution. Secondly, the n-torus topology creates unique constraints on the cell cycle, as the process of cell division transforming one cell into two has to eventually restore not just cell volume but also this unique cellular topology.

Topologically, the division of an n-torus cell would require significant rearrangement of membrane architecture. Importantly, these rearrangements take place within the confinement of the "outer theca" wall which largely conserves total apparent cellular volume and hydrodynamic profile while the associated vacuole and entangled cytoplasmic network divide(Fig. S1A) [57]. The topology undergoes a complete rearrangement at the point of cell division. After partitioning into two distinctly visible cells inside the theca, we observe a rapid breakdown of the wall. This dissolving wall eventually bursts and ejects the daughter cells, possibly driven by a hydrostatic pressure buildup(Movie S4,S5). This separation is immediately followed by a rapid inflation event of both daughter cells, which increase their volume 3-6 fold over 15 minutes(Fig. 2A,B).

Finally, for the vacuole and the cytoplasm to persist together despite inflation and division cycles, these two topological objects must remain linked together. This is clearly visible as cytoplasmic tunnels that pass through the vacuole geometry from one side to another. This can be further quantified as a linking number that ensures that no deformation of the geometry of cytoplasm or vacuole can separate the two.

Extracellular calcium triggers inflation

How would such a dramatic change in cellular architecture be choreographed? For cells, maintaining the intracellular osmotic differential is a critical aspect of cellular homeostasis and the task of many families of pores, channels, and pumps under control of different signaling networks [20, 49]. Attempting to understand which components might be involved in inflation, we used known channel interfering agents to perturb these proteins.

Inflation was recorded in cell populations at the beginning of their conditioned light cycle and quantified with projected 2D cell areas as a proxy for volume. In seawater of salinity 36 ppt, specific gravity 1.027, inflation results in a projected area growth of arouund 2.5 fold over a total observed time of 240 minutes. Supplementing the artificial seawater medium with 3mM of the calcium chelator EGTA completely stalls this inflation process with daughter cells maintaining their condensed volume through thecal wall breakdown(Fig. 2C, Movies S7,S8). Other calcium channel blockers such as Cobalt also inhibit inflation(Fig. S2, Movie S9). In addition, we noticed if the cell wall is compromised with a micro-pipette before natural breakdown, exposing the daughter cells to seawater, inflation will prematurely begin. These daughter cells conform to the profile of the mother's theca until enough internal pressure is built up to escape(Movie S11.) This suggests calcium, or a related signal, is actively excluded from the extracellular space until degradation of the cell wall is complete.

As calcium is a universal messenger, in developmental processes as well as size control, it is consistent with use as a signal to induce volume change. To more directly test the role of calcium, cells were placed in isotonic seawater medium prepared without calcium and allowed to progress through normal cell division. These cells, as with the EGTA treated cells, maintained condensed volumes through cell wall breakdown. Importantly, the cells remain viable, as when a bolus of calcium chloride solution is added to the media after the hours of starvation cells begin the inflation process within 60 seconds, and complete volume increase in the usual time window of 15 min(Fig. 2G). The final inflated size is less than the calcium replete cells, which is unsurprising considering calcium's role in other critical cell activities. Thus with calcium ions chelated from replete seawater, or with artificial seawater prepared without calcium, the mechanism initiating rapid volume increase is inactive, suggesting inflation is somehow actively regulated by components in the cell membrane.

Diffusive processes are often not sufficient for the translocation of large volumes of water across membranes. However, numerous processes require such flux [1, 8]. In metazoans, many processes including retinal and renal function, rely on channel proteins called aquaporins which can move up to 3×10^9 molecules of de-ionized water per second [28, 65]. Expression of aquaporin protein in a Xenopus oocyte is enough to swell these millimiter sized cells over 1.5 fold in a few minutes before they rupture. In addition, many plant processes such as pollen tube elongation, another example of rapid cell expansion under control a calcium gradient, and leaf movement, also require such selective movement of de-ionized water [19, 26, 33, 42]. As these molecules appear to be great candidates for an coordinated influx of low density ballast, we looked to confirm the presence of aquaporins in these dinoflagellates.

For this we assembled a working de-novo transcriptome for *Pyrocystis noctiluca* using Iso-seq long-read sequencing on the PacBio platform. When compared

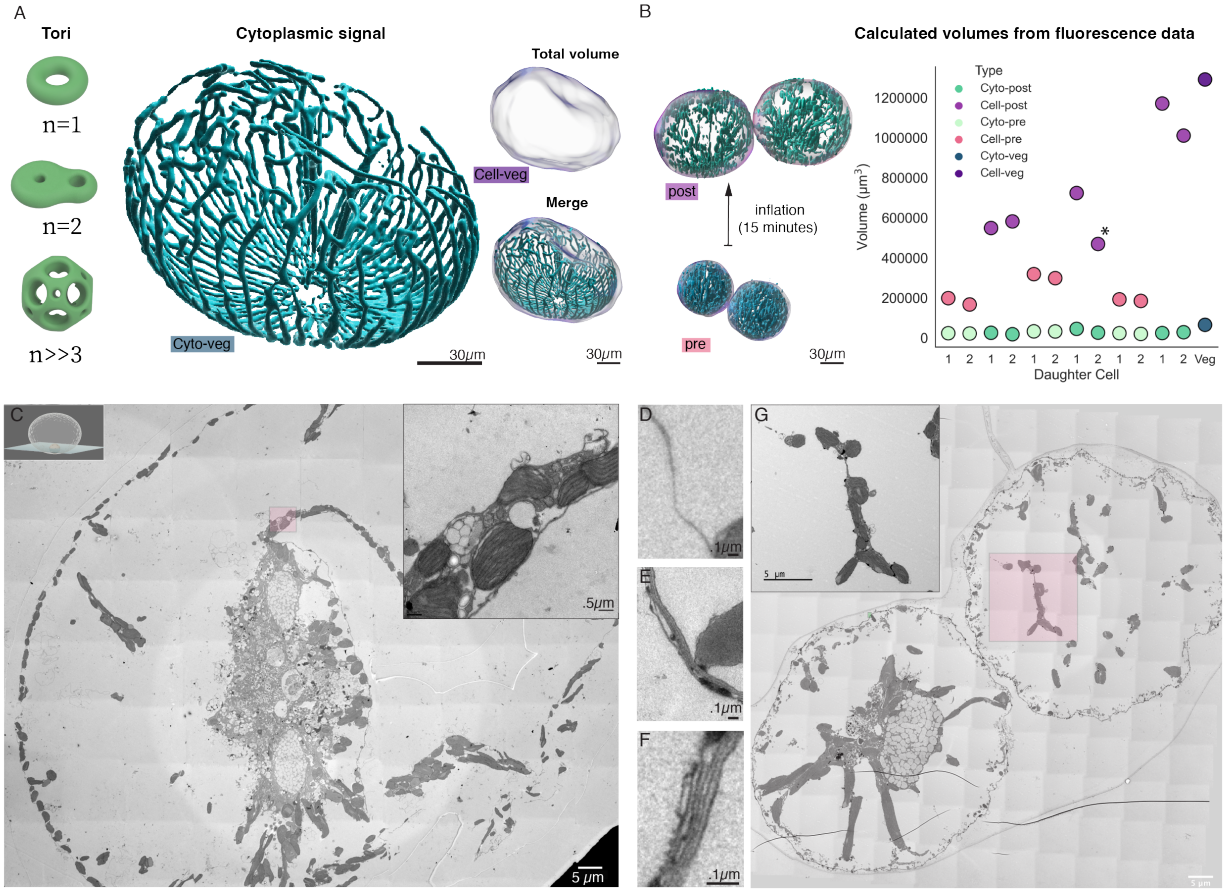

FIG. 3. **Cellular architecture in 3D**. A)Pyrocystis's cytoplasm is organized into a reticulated network that surrounds, and transects, the large inner vacuole. This can be described as an 'n-torus', where 'n' is the number of holes in the manifold-in this case the membrane bound cytoplasm. Such a structure allows for large cell volume changes without dilution or concentration effects on cytoplasmic contents. B) Quantification of cytoplasmic and cellular volumes before and after inflation in 3 pairs of dividing cells. Mature vegetative cell for comparison. 'Cyto' refers to cytoplasmic autofluorescence signal, 'Cell' refers to total cell volume. * cell temporarily drifted out of frame. Division results in a large increase of total cell volume while the volume of the cytoplasmic network is mainly conserved. C) Electron micrographs display the highly jammed composition of the cytoplasmic network. Inset highlights the membrane-bound organelles within a cytoplasmic filament. D) A mature cell is bound by a single contiguous membrane. (E,F) The membrane in an uninflated daughter cell appears as a laminated structure of 5-8 membrane layers. This could enable large and rapid increases in surface area. G) Dividing cells appear to have a compressed cytoplasmic filament network. Inset highlights such a membrane bound filament. All reported volumes are in µm

to known aquaporins across the tree of life the *Pyrocystis noctiluca* transcriptome encoded several proteins identified as aquaporins(Table. 1, Fig. S4). Using AlphaFold for protein structure prediction, several homologous sequences revealed canonical 6-pass Aquaporin structures (AQP1) along with other conformations such as the pollen-specific NIP4 [31]. NIP4-like hits are intriguing as these proteins are crucial to the hydration and vacuolation of pollen during development, a process requiring rapid volume increase [19](Fig. S4). The presence of these channels and numerous mechano-sensitive, voltage-sensing, and rectifying channels display a capable toolkit for size regulation in dinoflagelletes. This lays the foundation for unraveling molecular players and regulatory processes that enable cell inflation only after post-division-critical to the life-cycle of this cell.

Cells evading the gravitational trap

Our observations motivate a framework within which we understand the sedimentation physics of the cell undergoing various phases of its cell cycle. Unlike swimming at low Reynolds numbers [53, 58] where changes in the configuration of an organism leads to swimming strokes, in the non-motile cell under consideration activity manifests through changes in its internal state (cell cycle clock) which leads to a dynamic buoyancy. Here we aim to derive a single equation that captures the dynamics of cellular behavior during the entire cell cycle.

As described in (1) cellular behavior is both a func-

tion of cell size, cell density, and surrounding sea water density. All three parameters change during a cell cycle-radius and density due to internal physiology of the cell as it undergoes a complete cell cycle going from one cell to two-and seawater density due to the vertical stratification of the ocean. Considering the fact that our system includes active regulation of buoyancy (1) through a time-dependent internal state of the cell (cell cycle), we define a non-dimensional variable $\phi = \alpha t/nT_c$ where t/T_c is the time scaled by the total time period of the cell cycle (~ 7 days) and $n = 1, 2, 3..$ is the number of cell cycles. We have introduced activity through a simple constant parameter α, which drives the cell cycle at a constant rate α/T_c. Thus all the internal degrees of freedom of a cell are dependent on ϕ which simply quantifies the stage (phase) at which the cell is during its cell cycle. In the depiction of the relevant phases of the cell cycle(Fig. 4A), we arbitrarily assign ϕ to be zero at the start of cell inflation (starting at the moment two daughter cells break open out of the thecae of mother cell) and continuous through cell growth, pre-division, and duplication. ϕ is reset as a cell completes its cell cycle in T_c.

We map the time in equation (1) to the phase coordinate ($t \to \phi$) and non-dimensionalize (1) using the length of the daughter cell $L = r_{min}$, and the sedimentation time scale $T = 9\mu/(2g(\rho_{cy} - \rho_{vac})r_{min})$. Redefining $\tilde{r} = r/L$ and $\tilde{z} = z/L$ gives the equation of motion completely in terms of $\tilde{z}$ and ϕ coordinates,

$$\frac{d\tilde{\mathbf{z}}}{d\phi} = \frac{T_c}{\alpha T}\tilde{r}(\phi)^2 \left[\rho_{eff}(\phi) - \rho_{sw}(z)\right], \tag{3}$$

where the effective density $\rho_{eff}(\phi)$ given by the expression (2) is a function the internal state ϕ of the cell (Fig. 4A) and is independent of the precise geometry of the cytoplasm; which indeed has a non-trivial architecture (Fig. 3), and $\rho_{sw}(z)$ captures the pycnocline-the increase in sea water density as a function of depth z. Thus (3) can be seen as describing the dynamics of cell behavior captured in cell height, as a function of a complete cell cycle in an ocean sculpted by the pycnocline. Although fluid turbulence is universally present in marine ecosystems [22], turbulent mixing in the vertical direction is suppressed in regions away from the boundaries of the fluid (air-water and land-water interface) [39]. With the current focus to understand the deterministic part of the dynamics [equation (3)], we start with the underlying assumption of vertical flow velocities being negligible.

Deriving the full dynamical behavior of a cell during an entire cell cycle (ϕ ranging from 0 to 1), however, requires a priori knowledge of $\rho_{eff}(\phi)$, throughout the cell cycle. We approach this problem with a simplifying assumption considering two critical stages in the cell cycle where large scale density change occurs (Fig. 4 A)-first, the fast time scale ($\Delta T_B/T_c$) of rapid ballooning during which the cell density drops sharply due to intake of pure water, and second-a slow time scale ($1 - \Delta T_B/T_c$) process of cell growth where cell mass accumulates via production of cytoplasmic content and the density grows gradually to the number prior to cell division. This is also where controlled influx/efflux of salts would further regulate the buoyancy of the vacuole. Because a cell cycle, by definition, is a closed process where a single cell must produce two "identical" cells - it is required that the value of fast density decrease followed by slow density increase ends up within reasonable proximity of each other for a cell to not loose or gain mass in successive cycles.

To get the analytical expression for density variation during ballooning, we turn to experiments for the temporal profile of cell radius during ballooning ($\phi \ll 1$) – (Fig. 2) the volume of the vacuole V_{vac} is seen to increase dramatically and then saturates. This can be physiologically achieved by selectively taking in water through aquaporins. As discussed above; we find this rate of inflation by taking in water feasible with known aquaporin flux dynamics (rate of water molecules that a said channel can take in per unit time). This selective intake of water from the ambient sea water, via selective permeability of aquaporins, allows cells to dramatically affect buoyancy. From the experimental data, we can approximate the change of radius as an inverse tangent function between the cell radius r and cell phase ϕ,

$$\tilde{r}(\phi) = 1 + \frac{2}{\pi}\left(\tilde{r}_{max} - 1\right)\tan^{-1}\left(\frac{T_c\phi}{\alpha\Delta T_B}\right), \tag{4}$$

where $1/\alpha\Delta T_B = 0.0032$, $r_{min} = 48.77\mu m$ and $r_{max} - r_{min} = 18.6\mu m$, comes from experiments. The qualitative features of our theoretical result will be independent of this particular choice of Sigmoidal function.

In equation (4) a stretched coordinate $\Phi = \phi/\delta$ appears when we define $\delta \equiv \alpha\Delta T_B/T_c$ as the phase in ϕ where inflation happens. Since experimentally observed $\delta \ll 1$, it can be naturally considered as forming a boundary layer [7] of thickness δ in the temporal density profile near $\phi = 0$.(Fig. 4B) We define behavior inside this boundary condition in time as "inner" which is equivalent to an inflation phase and outside this time as "outer" or growth/pre-division phase. Thus, from equation (3) the density in the inner region (inflation phase) where $\Phi = \mathcal{O}(1)$, is given by

$$\rho_{inner}(\Phi) = \frac{\rho_{cy} - \rho_{vac}}{\left(1 + \frac{2}{\pi}\left(\tilde{r}_{max} - 1\right)\tan^{-1}(\Phi)\right)^3} + \rho_{vac} \tag{5}$$

The rate of cell density increase during growth phase might take many forms, but continuity of cell cycle parameters requires that the daughter cell gains cytoplasmic mass equivalent to a mother cell during a single cycle. Here we assume linear increase in effective cell density during the growth phase after inflation, which we call outer (growth phase) region $\phi \gg \delta$, given by

$$\rho_{outer}(\phi) = \gamma_0\phi + \gamma_1 + \mathcal{O}(\delta^2). \tag{6}$$

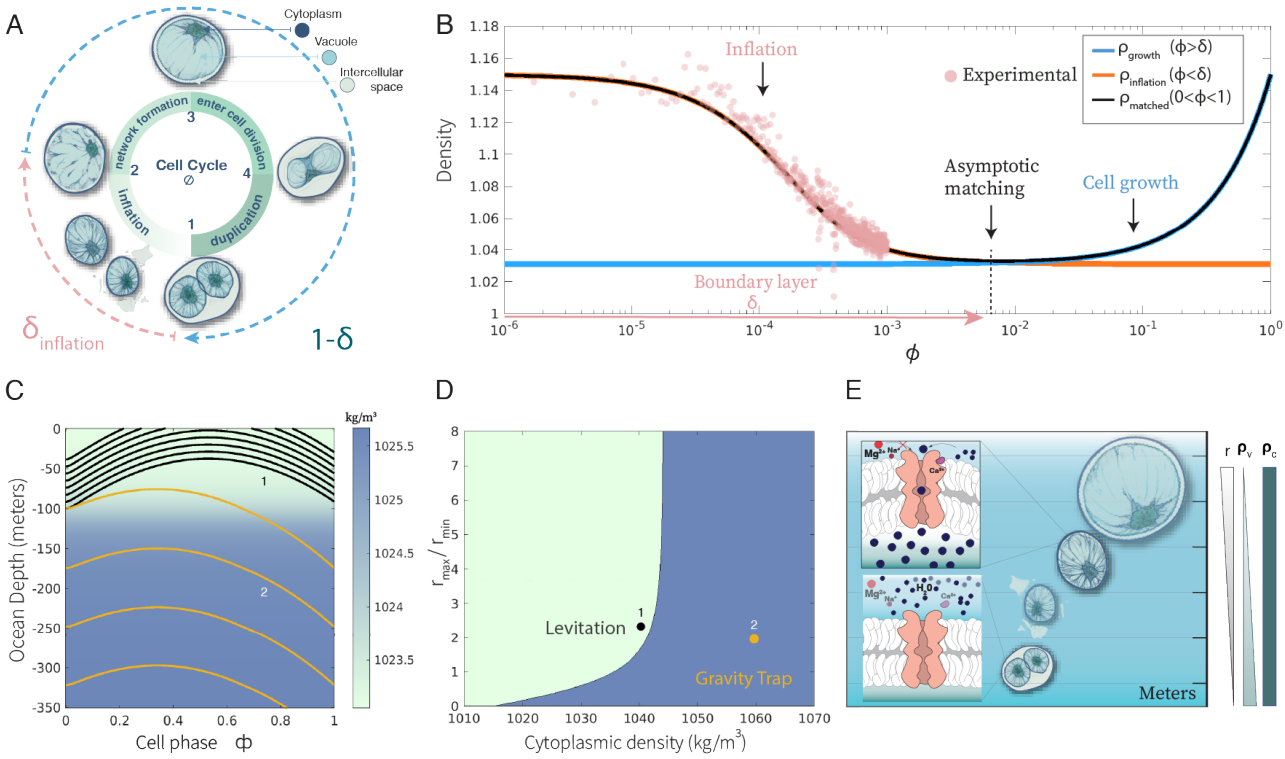

FIG. 4. **A model for inflation-based motility**.A)Pyrocystis undergoes numerous geometrical membrane transformations throughout its life-cycle while maintaining a general ellipsoidal form-factor to its cell-wall. 1.On cell-wall breakdown daughter cells quickly expand. 2. This material becomes organized into a reticulated network over the next few hours. 3. The mature Pyrocystis cell maintains a large vacuole and distributed cytoplasmic network for around 96 hours. 4.Division begins with a reorganization of the network and vacuole. This 'bowtie' shape eventually forms 2 spherical daughter cells. B) Comparing the asymptotically matched effective density in equation (7) with the experimentally observed density in the inflation phase, gives $\rho_{cy} = 1150 kg/m^3$ and $\rho_{vac} = 1010 kg/m^3$ with a boundary layer of thickness δ. C) Numerical solution of equation (8) using a measured pycnocline (shown as colorbar) from the *HOT317* cruise describing trajectories of two cells, the white uses inflation to decrease density and achieves levitation, rising in the water column. The yellow cell is beyond a critical density, wherein inflation cannot overcome the gravitational trap, thus it sinks into the abyss. D) Phase diagram with a critical density boundary beyond which even extreme inflation cannot counter downward gravitational pull, defining the gravity trap (blue region). The circles 1 & 2 corresponds to the levitating and trapped trajectories in C) respectively. E)Proposed role of selective molecular import in escaping a gravity trap. At the completion of cell division, the two daughter cells have greatly reduced vacuoles compared to mature cells. Without positively buoyant ballast they sediment to the lower euphotic zone. An unknown cue induces cell wall breakdown which then exposes the membrane to seawater. Calcium then binds and activates channels, including aquaporins, to import water into the vacuole. This rapidly increases cell volume while greatly reducing sedimentation velocity.

Asymptotic matching of the inner (inflation) and outer (growth) densities at the edge of the boundary layer [7], $\lim_{\Phi\to\infty} \rho_{inner}(\Phi) = \lim_{\phi\to 0} \rho_{outer}(\phi)$, gives the intercept $\gamma_1 = \rho_{vac} + (\rho_{cy} - \rho_{vac})/\tilde{r}^3_{max}$ in (6), and the constraint of periodicity on all cell cycle parameters gives the slope $\gamma_0 = (\rho_{cy} - \gamma_1)/(1-\delta)$. Carefully combining (7) and (6) gives the effective density that is valid in the full domain ϕ of the cell cycle,

$$\rho_{eff}(\phi) = \rho_{inner}(\phi/\delta) + \rho_{outer}(\phi) - \gamma_1. \qquad (7)$$

With these ingredients in (3), the dynamical equation in the $\tilde{z} - \phi$ space (defined as the solution phase for where a cell is in height z as a function of its cell cycle) takes the form

$$\delta \frac{d\tilde{z}}{d\phi} = -\frac{\Delta T_B}{T}\left(\frac{1}{\tilde{r}(\phi)} - [\beta(z) - \Gamma\,\phi]\,\tilde{r}(\phi)^2\right). \qquad (8)$$

Here $\Delta T_B/T$ is the ratio of ballooning time scale to sedimentation time scale, $\Gamma \equiv \gamma_0/(\rho_{cy} - \rho_{vac}) = 1 - \tilde{r}^{-3}_{max}$ is the measure of relative density reduction due to ballooning. A non-dimensional density parameter $\beta(z) = (\rho_{sw}(z) - \rho_{vac})/(\rho_{cy} - \rho_{vac})$ captures the external environment through the pycnocline – the increase in sea water density ρ_{sw} as a function of depth z, and internal cell parameters through vacuole density, and the cytoplasmic density. We have thus constructed a single differential equation which captures

the settling behavior throughout the cell cycle, with simplifying assumptions about the relevant stages of the cell cycle. This simple 1D model incorporates a wide range of length (cell radius approx. 50 microns to ocean stratification depth approx. 100 meters) and time (ballooning approx. 10 mins to cell cycle approx. 1 week) scales, while coupling the physical and biological components of these ecophysiological dynamics.

In equation (8) a small parameter δ multiplies with the derivative, and therefore the ballooning event can be mathematically treated as a singular perturbation to the dynamics [7]; thanks to the "abrupt" ballooning of the cell [see Fig. 4 B]. It is thus amenable to a singular perturbation analysis in which the inner (inflation phase) solution, to leading order, is the solution to

$$\frac{d\tilde{\mathbf{z}}}{d\phi} = -\frac{T_c}{\alpha T}\left\{\frac{1}{\tilde{r}} - \beta\tilde{r}^2\right\} \equiv -\frac{T_c}{\alpha T}V_B, \tag{9}$$

which has a fixed point in non-dimensional velocity $V_B = 0$ at $\tilde{r} = \beta^{-1/3}$, at which cells become neutrally buoyant, implying that via ballooning (increasing $\tilde{r}$) cells can steer themselves to rise from a sinking fate; consistent with our field observations(Fig. 4 A-E). Since the lifetime of the ballooning event δ is negligibly small compared to the total transit time of the organism, only the outer (growth phase) solution of equation (8) is ecologically relevant. In a constant pycnocline approximation, the outer solution to (8), to leading order in δ, becomes

$$\tilde{z}(\phi) = z_0 - \frac{T_c}{\alpha T}\left(\frac{1}{2}\Gamma\,\tilde{r}_{max}^2\,\phi^2 + V_B\,\phi\right) + \frac{T_c}{\alpha T}V_B\,\delta + \mathcal{O}(\delta^2), \tag{10}$$

where V_B is the velocity immediately after ballooning, given by (9) with $\tilde{r} = \tilde{r}_{max}$ [see Fig. 2 E], and z_0 is the ocean depth at which the first cell cycle begins. The ecophysiological and mathematical relevance of ballooning based migration also enables resetting of the "slingshot" and adding residual corrections to the trajectory as a perturbation expansion in δ. The notable outcomes of this analysis are:

1) Criticality – equation (10) is a parabola in (ϕ,z) plane with the vertex at $\phi = (1-\beta\tilde{r}_{max}^3)/(1-\tilde{r}_{max}^3)$. Setting $\phi = 1/2$ gives the critical ballooning radius required for escaping the gravity trap (gradually rise in the long time scale of multiple cell cycles), $\tilde{r}_c \sim (\beta - 0.5)^{-1/3}$, which diverges as $\beta \to 0.5$ with a critical exponent 1/3, giving the condition

$$\rho_{cy} + \rho_{vac} \leq 2\rho_{sw} \tag{11}$$

on relevant densities for an escape. This implies that beyond a set of critical parameters it is not possible to escape the "gravity trap" and eventually a cell will sink if no upwelling brings it up (Fig. 4C, D), thus formally allowing gravitational force to apply selection pressure in the evolution of phytoplankton in this framework.

2) Effective inertia – for a constant pycnocline, equation (8) can be mapped to the equation of a projectile shot vertically $m\,d^2\tilde{z}/d\tilde{t}^2 = -\alpha$, with an effective mass or inertia $m \equiv T_c/(T\Gamma\tilde{r}_{max}^2)$ which depends on the ballooning radius and effective drive α which is defined as a constant force that drives the cell cycle clock in Fig. 4A. This effective inertial dynamics in a Stokesian regime comes from internal degrees of freedom actively driven in the cell. This seemingly exclusive possibility also appears in the dynamics of micro-swimmers [11, 70] and passively sinking particles with internal degrees of freedom [15].

To draw the $z-\phi$ phase in its completeness we numerically integrate (8), using the pycnocline measured by CTD during the HOT 317 cruise, $\rho_{sw} = 1024.3 + 0.9\tan^{-1}0.05(z-107.8)kg/m^3$, and assuming only fresh water permeates through the membrane $\rho_{vac} = 1000kg/m^3$. We find escaping and trapped trajectories in Fig. 4C, for small and large values of cytoplasmic density ρ_{cy} respectively. This clearly demarcates a space of parameters that can lead to a cell being perpetually suspended while navigating the water column vertically as compared to another cell population which will eventually sink to the bottom of the ocean. It is interesting to note that in our calculations this phase space becomes unbounded and rises sharply around the cytoplasmic density $1040mg/cm^2$(Fig. 4D).This critical behavior does not depend on the initial vertical position of the cell, thus the phase diagram is robust to the vertical flow fluctuations in the ocean.

The ballistic motion resulting from the dynamics of buoyancy control presents a unique advantage for organisms that demonstrate long-distance migrations such as pyrocystis cells. Because this mechanism is robust to any orientational noise/diffusion and drift caused by fluid shear, organisms can maintain course over long distances as compared to classical swimmers that are highly sensitive to cell orientation. The framework presented above can be extended to a number of aquatic organisms experiencing a downward pull and provides insights into organization of cell cycle in context of vertical migration. Thus ballooning in a cell in context of a vertical migration can be considered as a necessary *slingshot* mechanism needed to escape the "gravity trap".

Discussion

Although life is common in earth's atmospheres, on land, and in aquatic environments, our oceans provide the largest biosphere on our planet, where complex life evolved over billions of years. Oceans provided a unique and vertically stratified ecological podium where every parameter such as pressure, temperature, light, salinity, density, turbulence and nutrients vary continuously as a function of depth. Thus an up and down migration over only a hundred meters can take an organism into vastly different ecological conditions.

A diversity of organisms have evolved adaptations that enabled cells to survive as these vertically stratified ecosystems served as an evolutionary force. Canonical cellular functions like environmental sensing, osmoregulation, and cell size control, mechanisms ubiquitous in all living cells, originated as adaptations to ecological challenges first posed by life in these seascapes. Integrating these adaptations was necessary not only for homeostasis but for motility. For *Pyrocystis noctiluca* and cells like it, fine control of osmoregulatory and electrochemical machinery dictates how and where one exists in the water column. Using *Pyrocystis noctiluca* as a model system, we build up on the insightful work done over the last century to establish a direct link between ecological and physiological parameters such as ocean depth and cell cycle; where cell size controls a population level distribution in the water column.

We propose to link these parameters using a mathematical framework that emphasizes the importance of cellular topology and cell cycle. We demonstrate that an n-genus toroidal geometry enables a rapid 10-fold inflation of the cell volume without dilution of its biochemical machinery. This emphasizes the role of understanding cell size in context of its physiology and the need to study cell geometry in conjunction with overall size. Diurnal mobility of this cytoplasmic network confronts fundamental diffusive limits which can easily depart from spherical models of cellular forms. This topology puts further constraints on organelle transport within a cell, such as plastids traveling in a reticulated network inside the cell in a daily extension/retraction cycle.

Buoyancy based mechanisms for levitation are versatile and effective in a vertically stratified ocean, and are reported in inhabitants ranging from single celled plankton to large cephalopods; also appearing in engineering solutions for submersibles [69]. Meter-scale movement at negligibly small Reynolds numbers sets insurmountable demands for microscale flagellar swimmers [56], with the flagellar and ciliary motility being highly sensitive to orientational noise from shear in the fluid (turbulence). The mechanisms of buoyancy control, however, do not depend on cell orientation, thus providing a robust means for a ballistic long-distance journey.

In a comparative context, we also observed a morphologically similar cell like Noctiluca scintillans, a heterotrophic plankton, maintains an unwavering positive buoyancy(Fig. S6, Movie S10). As Noctiluca cells accumulate nitrogen from consuming phytoplankton they need not traverse great depths or balance this with presence in sunlit waters. They undergo a much more gradual fission process to divide, suggesting that the rapid inflation process could be linked with the control of life at depth.

Our transcriptomics data introduces candidates we can follow with sensors and effectors responsible for this migratory behavior, both in the 'inner' and 'outer' phases of the life cycle. More specifically, the discovery of aquaporins and an array of sensors, channel proteins, and kinases leaves open the opportunity to describe a robust biochemical network behind a complex and ecologically relevant behavior [30]. Aquaporins have been shown to be directly sensitive to environmental conditions such as pH and Calcium, which is consistent with our experiments showing calcium exposure to be critical for daughter cell expansion [46, 47]. The labeling of aquaporins in diatoms has recently revealed these environmental inputs to be critical for these fellow migrators [41].

The obvious lack of positive buoyancy covering the 'outer' phase of the cell cycle in our lab strain might arise from adaptive loss over nearly 2,500 generations spent without depth-driven ecological pressure (given a 7 day cell cycle and strain isolation in November of 1977). This also motivates further comparative molecular study with the wild strain. Direct labeling of cellular components within live Pyrocystis proved to be challenging due to impermeability of Dinosporin cell wall. Dinosporin maturation bounds the complex vacuolar/cytoplasmic geometry and serves to limit daughter cell expansion. Further work is required to decipher unique molecular players behind this cell wall that forms an extremely resistant structure. It's timed and rapid degradation serves to reset the slingshot by inducing inflation(Movie S5).

The present theoretical framework offers a dynamical system perspective to the life of a seemingly non-motile plankton suspended in the ocean; where motility comes from active buoyancy control rather than a conventional swimming mechanism [53, 58]. Our theory stitches together widely separated length and time scales, resulting in a minimal 1D model that incorporates both the physical and cell-physiological aspects of this reduced ecosystem. It offers a framework in which gravitational pull can formally operate as a selection pressure in the evolution of marine plankton [density inequality as in equation (11)]. In future work, the dynamical equation (8) can be further embellished to account for a broader group of ecological parameters including variation in salinity, temperature and explict cellular feedback. Although the mathematical forms of ρ_{inner} and ρ_{outer} [equation (7) & (6)] comes from observations specific to *Pyrocystis noctiluca*, the matched asymptotic approach presented here is likely generalizable to a richer class of plankton with cell cycle phases involving multiple boundary layers, and non-linearities in the growth phase. The current model presents a deterministic dynamical system. Since fluid turbulence is a universal feature present in all marine ecosystems, we can further incorporate it in our models either as stochasticity in equation (8) or more elaborately by coupling equation (8) with the Navier-Stokes equation for the fluid flow [22].

The daily planktonic migrations constitute the 'biological pump' and fix about 40-60% of earth's carbon

emissions, a holistic understanding of this process and anthropogenic impact on the resulting carbon flux will only become ever more important[12, 14] for potential remediation.

Methods

Obtaining dinoflagellates in the field Pyrocystis cells were first obtained from a CTD rosette bottle triggered at a depth of 75m. When foul weather prohibited further casts, vertical plankton tows were done from 25-35m with a 20 micron mesh plankton net at a max speed of 1kt. Presence of Pyrocystis noctiluca in the sample was confirmed via imaging on a flow-through Planktoscope instrument. Cells were then isolated on a dissection microscope and placed in filtered underway water. 5 micron polystyrene beads were added to the media prior to loading into the sample stage to mark flow fields for later PIV correction.

Cell Culture Pyrocystis noctiluca (CCMP732) were ordered from Bigelow Labs and expanded in F/2 media(-Si) prepared using artificial seawater (reef salts) at a salinity of 37%, specific gravity 1.027. Cells were cultured at 21°C under cool white fluorescent light at 2500 lux. Media was refreshed every 2 weeks to maintain proper salinity. Cells were expanded every 6 weeks to minimize accumulation of cell debris.

Pyrocystis division assay Dividing Pyrocystis cells (with 2 daughter cells visible inside the cell wall) were isolated on a dissection scope, washed in fresh media, and placed in 5ml of F/2. Mature cells were included as a proxy of cell viability, as plasmolysis is much more apparent in the mature cells. EGTA was added from a .5M stock solution. DI Water was added as mock to control cells. For the calcium depletion experiment, cells were sorted, washed, and placed in F/2 media prepared with calcium-free artificial seawater prepared according to the Cold Spring Harbor protocol. The calcium bolus was from a .5M CaCl stock solution.

Image Processing *Bulk Assay* To quantify the area increase in a population of dividing cells, a custom model was generated within Cellpose v2.0 [62]. This was done by updating the pretrained 'Cyto2' model with an annotated mask layer drawn in the Napari viewer containing around 150 dividing Pyrocystis cells. Unique labels were then applied to each cell in the mask using OpenCV. Projected cell area was then calculated using the region properties function in OpenCV. Cells were then morphologically categorized according to cell state. Dead or Plasmolysed cells were excluded from analysis at this stage and classified as 'Lysed'. *Vertical Tracks* To quantify the area in sedimenting cells the Watershed algorithm was applied using OpenCV after simple morphological operations to remove background. In frames where the cell drifted out of focus in Y, no volume change was assumed between the current and previous frame.

Vertical Velocity Measurements Tracking experiments on the R/V Kilo Moana were performed by securing the microscope with straps to a fixed laboratory table with ambient temperature between 20-22°C. Since the vessel's roll during foul weather introduced flow into the annular chamber, a plug was used to suppress any motion induced flows. This essentially limited field measurements to the circumference of a circular stage. In the lab, the microscope was secured within a temperature and light controlled enclosure (21°C) to an optical table. To quantify the vertical velocities of cells in the tracking microscope, background flows from thermal fluctuations or other movement were first subtracted using tracking beads to mark the flow-field and OpenPIV software. The 'Gravity Machine' analysis suite was used to determine sedimentation rate as described previously in [34, 35]. A high frequency filter was used for comparison of separate tracks. Raw traces vs. filtered data is presented in supplementary materials.

Light sheet imaging Light sheet imaging of Pyrocystis cells was done on a Luxendo InVi SPIM instrument using a Nikon CFI Apo 25x W 1.1 NA objective with optivar set at either 31.3 or 62.5X total magnification. The sample was maintained in a water bath held at 21°C for the duration of each experiment. Image processing was done in Imaris. Isosurfaces were created for the fluorescence signal within the network and volumes were subsequently calculated. Since the cell wall has no fluorescent signal, a surface was projected on the exterior of the network encompassing the entire cell. The total calculated volume of this surface was used as a proxy of total cell volume. Tori in Fig. 3 were generated in Fusion 360.

Long-term imaging Long-term imaging of the Pyrocystis life-cycle was done on a 'Squid' imaging system within a peltier controlled chamber kept at 21°C [37, 38]. The cells were imaged in a 50mm Pelco glass bottomed dish that was sealed with a glass coverslip after filling the chamber with F/2 medium. A LED panel was used to simulate the 12/12 light dark cycle.

Electron Microscopy Electron microscopy was done at the UC Berkeley electron microscopy core facility. Cell morphology was compared between samples fixed chemically and by high pressure freezing. Rapid chemical fixation provided the most reproducible results with minimal damage to overall morphology. Fixation was done with addition of 2% Paraformadahyde, 3% Gluteraldahyde to the media. Use of the Pelco BioWave was essential to avoid retraction of the cytoplasmic network or plasmolysis. The Pelco was used at 150watts, switched on for 1 minute with vacuum off, 1 minute with vacuum on, switched off for 1 minute with vacuum on, and finally 1 minute switched on with vacuum engaged. Samples were then stained and processed into resin before sectioning.

RNA preparation for Long-Read sequencing Around 5,000 cells were collected in a 40µm cell strainer and washed with 10mls of sterile filtered F/2

culture medium. Cells were then quickly scraped off the filter with a metal spatula and placed directly into 1ml of Trizol reagent where they were further homogenized for 30 seconds with a plastic pestle attached to a power drill. RNA was then purified on a column according to the PureLinkTM Micro Kit protocol. RNA quality was assessed with a BioAnalyzer run using both the 'Plant RNA pico' and 'Eukaryote RNA pico' protocols. The RNA peaks on the electropherogram were considered high quality and processed further for sequencing by PacBio.

Protein structure prediction The transcriptome assembled from the long-read sequencing was first aligned against all entries in the UniProt/Swiss-Prot database. High quality alignments were then loaded into Alphafold using ChimeraX, and figures were generated using the same [50].

Acknowledgments

We thank the crew of R/V Kilo Moana and cruise *HOT317* for enabling the entirety of the field work. We thank Rama Govindarajan for fruitful discussions on asymptotics.We thank Rebecca Konte for discussions and illustrations. We thank Scott Coyle for insightful comments on the work. We thank Vijay Ramani for expertise with analyzing and interpreting the PacBio data. We thank Deepak Krishnamurthy for his stimulating conversations and expertise on sedimentation. We thank Dane Maxfield for his generosity and expertise with the Luxendo microscope. We thank Danielle Jorgens and the Berkeley Electron Microscope facility for aid with processing and imaging. We thank all members of PrakashLab for comments and discussions throughout this work. AGL is supported by the Simons foundation. RC is supported by the HFSP Postdoctoral Fellowship. This work is supported by HHMI Faculty fellowship (MP), BioHub Investigator Fellowship (MP), Schmidt Innovation Fellowship (MP), Keck Foundation Research Grant and NSF CCC (DBI1548297).

[1] Peter Agre. The aquaporin water channels. Proceedings of the American Thoracic Society, 3(1):5–13, 2006.

[2] Valérie Andersen and Jacques Sardou. Pyrosoma atlanticum (tunicata, thaliacea): diel migration and vertical distribution as a function of colony size. Journal of Plankton Research, 16(4):337–349, 1994.

[3] David Antoine, Jean-Michel André, and André Morel. Oceanic primary production: 2. estimation at global scale from satellite (coastal zone color scanner) chlorophyll. Global biogeochemical cycles, 10(1):57–69, 1996.

[4] William W Baldwin, Richard Myer, Erika Anderson, and Arthur L Koch. Buoyant density of escherichia coli is determined solely by the osmolarity of the culture medium. Archives of microbiology, 164(2):155–157, 1995.

[5] Robert W Ballek and Elijah Swift. Nutrient-and light-mediated buoyancy control of the oceanic non-motile dinoflagellate pyrocystis noctiluca murray ex haeckel (1890). Journal of Experimental Marine Biology and Ecology, 101(1-2):175–192, 1986.

[6] Michael J Behrenfeld, Robert T O'Malley, David A Siegel, Charles R McClain, Jorge L Sarmiento, Gene C Feldman, Allen J Milligan, Paul G Falkowski, Ricardo M Letelier, and Emmanuel S Boss. Climate-driven trends in contemporary ocean productivity. Nature, 444(7120):752–755, 2006.

[7] Carl M. Bender and Steven A. Orzag. Advanced mathematical methods for scientists and engineers i: Asymptotic methods and perturbation theory. Springer, New York, 1999.

[8] Gheorghe Benga, Octavian Popescu, Victor I. Pop, and Ross P. Holmes. P-(chloromercuri)benzenesulfonate binding by membrane proteins and the inhibition of water transport in human erythrocytes. Biochemistry, 25(7):1535–1538, 1986. PMID: 3011064.

[9] RL Berg. Some conditions for the appearance of life on the earth. In The Origin of Life on the Earth, pages 169–171. Elsevier, 1959.

[10] Dolors Blasco. Observations on the diel migration of marine dinoflagellates off the baja california coast. Marine Biology, 46(1):41–47, 1978.

[11] Austen Bolitho, Rajesh Singh, and R. Adhikari. Periodic orbits of active particles induced by hydrodynamic monopoles. Phys. Rev. Lett., 124:088003, Feb 2020.

[12] Philip W Boyd, Hervé Claustre, Marina Levy, David A Siegel, and Thomas Weber. Multi-faceted particle pumps drive carbon sequestration in the ocean. Nature, 568(7752):327–335, 2019.

[13] Andrea K Bryan, Alexi Goranov, Angelika Amon, and Scott R Manalis. Measurement of mass, density, and volume during the cell cycle of yeast. Proceedings of the National Academy of Sciences, 107(3):999–1004, 2010.

[14] EL Cavan, EC Laurenceau-Cornec, M Bressac, and PW Boyd. Exploring the ecology of the mesopelagic biological pump. Progress in Oceanography, 176:102125, 2019.

[15] Rahul Chajwa, Narayanan Menon, Sriram Ramaswamy, and Rama Govindarajan. Waves, algebraic growth, and clumping in sedimenting disk arrays. Phys. Rev. X, 10:041016, Oct 2020.

[16] Malcom R Clarke, Erik J Denton, and John B Gilpin-Brown. On the use of ammonium for buoyancy in squids. Journal of the Marine Biological Association of the United Kingdom, 59(2):259–276, 1979.

[17] Natalie R Cohen, Matthew R McIlvin, Dawn M Moran, Noelle A Held, Jaclyn K Saunders, Nicholas J Hawco, Michael Brosnahan, Giacomo R DiTullio, Carl Lamborg, John P McCrow, et al. Dinoflagellates alter their carbon and nutrient metabolic strategies across environmental gradients in the central pacific ocean. Nature Microbiology, 6(2):173–186, 2021.

[18] EJ Denton and JB Gilpin-Brown. Floatation mechanisms in modern and fossil cephalopods. In Advances in marine biology, volume 11, pages 197–268. Elsevier, 1973.

[19] Juliana Andrea Pérez Di Giorgio, Gerd Patrick Bienert, Nicolás Daniel Ayub, Agustín Yaneff, María Laura Barberini, Martín Alejandro Mecchia, Gabriela Amodeo, Gabriela Cynthia Soto, and Jorge Prometeo Muschietti. Pollen-specific aquaporins nip4; 1 and nip4; 2 are required for pollen development and pollination in arabidopsis thaliana. The Plant Cell, 28(5):1053–1077, 2016.

[20] Frederick George Donnan. The theory of membrane equilibria. Chemical reviews, 1(1):73–90, 1924.

[21] RC Dugdale and JJ Goering. Uptake of new and regenerated forms of nitrogen in primary productivity 1. Limnology and oceanography, 12(2):196–206, 1967.

[22] William M Durham, Eric Climent, Michael Barry, Filippo De Lillo, Guido Boffetta, Massimo Cencini, and Roman Stocker. Turbulence drives microscale patches of motile phytoplankton. Nature communications, 4(1):1–7, 2013.

[23] Richard B Forward. Light and diurnal vertical migration: photobehavior and photophysiology of plankton. In Photochemical and photobiological reviews, pages 157–209. Springer, 1976.

[24] Lionel Guidi, Samuel Chaffron, Lucie Bittner, Damien Eveillard, Abdelhalim Larhlimi, Simon Roux, Youssef Darzi, Stéphane Audic, Léo Berline, Jennifer R Brum, et al. Plankton networks driving carbon export in the oligotrophic ocean. Nature, 532(7600):465–470, 2016.

[25] Alister Clavering Hardy. The plankton of the south georgia whaling grounds and adjacent waters, 1926-1932. Discovery Rep., 11:1–456, 1935.

[26] Peter K Hepler. Calcium: a central regulator of plant growth and development. The Plant Cell, 17(8):2142–2155, 2005.

[27] Jonathon Howard and RL Clark. Mechanics of motor proteins and the cytoskeleton. Appl. Mech. Rev., 55(2):B39–B39, 2002.

[28] Ingela Johansson, Maria Karlsson, Urban Johanson, Christer Larsson, and Per Kjellbom. The role of aquaporins in cellular and whole plant water balance. Biochimica et Biophysica Acta (BBA)-Biomembranes, 1465(1-2):324–342, 2000.

[29] Gregory C Johnson, Rick Lumpkin, Simone R Alin, Dillon J Amaya, Molly O Baringer, Tim Boyer, Peter Brandt, Brendan R Carter, Ivona Cetinić, Don P Chambers, et al. Global oceans. Bulletin of the American Meteorological Society, 102(8):S143–S198, 2021.

[30] Kenneth D Johnson and Maarten J Chrispeels. Tonoplast-bound protein kinase phosphorylates tonoplast intrinsic protein. Plant Physiology, 100(4):1787–1795, 1992.

[31] John Jumper, Richard Evans, Alexander Pritzel, Tim Green, Michael Figurnov, Olaf Ronneberger, Kathryn Tunyasuvunakool, Russ Bates, Augustin Žídek, Anna Potapenko, et al. Highly accurate protein structure prediction with alphafold. Nature, 596(7873):583–589, 2021.

[32] Norman Kahn and Elijah Swift. Positive buoyancy through ionic control in the nonmotile marine dinoflagellate pyrocystis noctiluca murray ex schuett 1. Limnology and Oceanography, 23(4):649–658, 1978.

[33] Alexander Krichevsky, Stanislav V Kozlovsky, Guo-Wei Tian, Min-Huei Chen, Adi Zaltsman, and Vitaly Citovsky. How pollen tubes grow. Developmental biology, 303(2):405–420, 2007.

[34] Deepak Krishnamurthy. gravitymachine-analysis-scripts. https://github.com/deepakkrishnamurthy/gravitymachine-analysis-scripts, 2020.

[35] Deepak Krishnamurthy, Hongquan Li, François Benoit du Rey, Pierre Cambournac, Adam G Larson, Ethan Li, and Manu Prakash. Scale-free vertical tracking microscopy. Nature Methods, 17(10):1040–1051, 2020.

[36] Guancheng Li, Lijing Cheng, Jiang Zhu, Kevin E Trenberth, Michael E Mann, and John P Abraham. Increasing ocean stratification over the past half-century. Nature Climate Change, 10(12):1116–1123, 2020.

[37] Hongquan Li, Deepak Krishnamurthy, Ethan Li, Pranav Vyas, Nibha Akireddy, Chew Chai, and Manu Prakash. Squid: simplifying quantitative imaging platform development and deployment. bioRxiv, 2020.

[38] Hongquan Li, Hazel Soto-Montoya, Maxime Voisin, Lucas Fuentes Valenzuela, and Manu Prakash. Octopi: Open configurable high-throughput imaging platform for infectious disease diagnosis in the field. 2019.

[39] Andreas Lorke and Frank Peeters. Toward a unified scaling relation for interfacial fluxes. Journal of Physical Oceanography, 36(5):955–961, 2006.

[40] AD Macknight and Alexander Leaf. Regulation of cellular volume. Physiological reviews, 57(3):510–573, 1977.

[41] Hiroaki Matsui, Brian M Hopkinson, Kensuke Nakajima, and Yusuke Matsuda. Plasma membrane-type aquaporins from marine diatoms function as co2/nh3 channels and provide photoprotection. Plant Physiology, 178(1):345–357, 2018.

[42] NAEL A McCarty and ROGER G O'Neil. Calcium signaling in cell volume regulation. Physiological reviews, 72(4):1037–1061, 1992.

[43] Craig R McClain, Andrew P Allen, Derek P Tittensor, and Michael A Rex. Energetics of life on the deep seafloor. Proceedings of the National Academy of Sciences, 109(38):15366–15371, 2012.

[44] J Keith Moore and Tracy A Villareal. Size-ascent rate relationships in positively buoyant marine diatoms. Limnology and Oceanography, 41(7):1514–1520, 1996.

[45] Luigi Naselli-Flores and Rossella Barone. Invited review-fight on plankton! or, phytoplankton shape and size as adaptive tools to get ahead in the struggle for life. Cryptogamie, Algologie, 32(2):157–204, 2011.

[46] Karin L Németh-Cahalan and James E Hall. ph and calcium regulate the water permeability of aquaporin 0. Journal of Biological Chemistry, 275(10):6777–6782, 2000.

[47] Karin L Németh-Cahalan, Katalin Kalman, and James E Hall. Molecular basis of ph and ca2+ regulation of aquaporin water permeability. The Journal of general physiology, 123(5):573–580, 2004.

[48] Patrick H O Farrell. How metazoans reach their full size: the natural history of bigness. COLD SPRING HARBOR MONOGRAPH SERIES, 42:1–22, 2004.

[49] J Th Overbeek. The donnan equilibrium. Prog. Biophys. Biophys. Chem, 6(1):57–84, 1956.

[50] Eric F Pettersen, Thomas D Goddard, Conrad C

Huang, Elaine C Meng, Gregory S Couch, Tristan I Croll, John H Morris, and Thomas E Ferrin. Ucsf chimerax: Structure visualization for researchers, educators, and developers. Protein Science, 30(1):70–82, 2021.

[51] Aude Picard and Isabelle Daniel. Pressure as an environmental parameter for microbial life—a review. Biophysical chemistry, 183:30–41, 2013.

[52] Albert J Plueddemann and Robert Pinkel. Characterization of the patterns of diel migration using a doppler sonar. Deep Sea Research Part A. Oceanographic Research Papers, 36(4):509–530, 1989.

[53] Edward M Purcell. Life at low reynolds number. American journal of physics, 45(1):3–11, 1977.

[54] John A Raven and Martina A Doblin. Active water transport in unicellular algae: where, why, and how. Journal of Experimental Botany, 65(22):6279–6292, 2014.

[55] DF Rolfe and Guy C Brown. Cellular energy utilization and molecular origin of standard metabolic rate in mammals. Physiological reviews, 77(3):731–758, 1997.

[56] Paul E Schavemaker and Michael Lynch. Flagellar energy costs across the tree of life. eLife, 11, 2022.

[57] Kyung Suk Seo and Lawrence Fritz. The cytoskeletal network during division in the marine dinoflagellates, pyrocystis lunula and p. noctiluca. Algae, 15(3):137–141, 2000.

[58] Alfred Shapere and Frank Wilczek. Geometry of self-propulsion at low reynolds number. Journal of Fluid Mechanics, 198:557–585, 1989.

[59] George N Somero. Adaptations to high hydrostatic pressure. Annual review of physiology, 54(1):557–577, 1992.

[60] Ulrich Sommer, Evangelia Charalampous, Savvas Genitsaris, and Maria Moustaka-Gouni. Benefits, costs and taxonomic distribution of marine phytoplankton body size. Journal of Plankton Research, 39(3):494–508, 2017.

[61] George Gabriel Stokes et al. On the effect of the internal friction of fluids on the motion of pendulums. 1851.

[62] Carsen Stringer and Marius Pachitariu. Cellpose 2.0: how to train your own model. bioRxiv, 2022.

[63] Elijah Swift and Valerie Meunier. Effects of light intensity on division rate, stimulable bioluminescence and cell size of the oceanic dinoflagellates dissodinium lunula, pyrocystis fusiformis and p. noctiluca 1 2. Journal of Phycology, 12(1):14–22, 1976.

[64] Elijah Swift, Marc Stuart, and Valerie Meunier. The in situ growth rates of some deep-living oceanic dinoflagellates: Pyrocystis fusiformis and pyrocystis noctiluca 1. Limnology and Oceanography, 21(3):418–426, 1976.

[65] AS Verkman. Role of aquaporin water channels in eye function. Experimental eye research, 76(2):137–143, 2003.

[66] Tracy A Villareal. Positive buoyancy in the oceanic diatom rhizosolenia debyana h. peragallo. Deep Sea Research Part A. Oceanographic Research Papers, 35(6):1037–1045, 1988.

[67] Tracy A Villareal and Fredric Lipschultz. Internal nitrate concentrations in single cells of large phytoplankton from the sargasso sea 1. Journal of Phycology, 31(5):689–696, 1995.

[68] Tracy A Villareal, Cynthia H Pilskaln, Joseph P Montoya, and Mark Dennett. Upward nitrate transport by phytoplankton in oceanic waters: balancing nutrient budgets in oligotrophic seas. PeerJ, 2:e302, 2014.

[69] M Worall, Alan John Jamieson, A Holford, Richard David Neilson, M Player, and Philip Michael Bagley. A variable buoyancy system for deep ocean vehicles. In Oceans 2007-Europe, pages 1–6. IEEE, 2007.

[70] Andreas Zöttl and Holger Stark. Nonlinear dynamics of a microswimmer in poiseuille flow. Phys. Rev. Lett., 108:218104, May 2012.

TABLE I. Relevant alignments from PacBio transcriptome assembly.

Protein	**Organism**	**Class**
AQP1CANLF Aquaporin-1	Canis lupus familiaris	Aquaporin
PIP2-3	Oryza sativa	Aquaporin
AQPAEDAE	Aedes aegypti	Aquaporin
NIP1NICAL	Nicotiana alata	Aquaporin
NIP42ARATH	Arabidopsis thaliana	Aquaporin
CDPKOORYSJ	Sativa subsp. japonica	Calcium-dependent kinase
CDPK2PLAFK	Plasmodium falciparum	Calcium-dependent kinase
MAPC1ARATH	Arabidopsis thaliana	Calcium-dependent kinase
KCC1AHUMAN type 1	Homo sapiens	Calcium-dependent kinase
CDPK2LAFK	Plasmodium falciparum	Calcium-dependent kinase
CAMK1ARATH CDPK-related kinase 1	Arabidopsis thaliana	Calcium-dependent kinase
CIPKJARATH	Arabidopsis thaliana	Calcium-dependent kinase